

Classification of Blood Cells with Convolutional Neural Network Model

Emrah ASLAN^{1*}, Yıldırım ÖZÜPAK²

¹ Dicle University, Silvan Vocational School, Department of Computer Programming, Diyarbakır, Türkiye

² Dicle University, Silvan Vocational School, Department of Electricity, Diyarbakır, Türkiye
(ORCID: [0000-0002-0181-3658](https://orcid.org/0000-0002-0181-3658)) (ORCID: [0000-0001-8461-8702](https://orcid.org/0000-0001-8461-8702))



Keywords: Convolutional Neural Network, White Blood Cell, Deep Learning, Artificial Intelligent.

Abstract

White Blood Cells are the primary blood cells that come from the bone marrow and are essential for constructing our body's defense system. Leukopenia is a disorder where the body's capacity to fight off infections is compromised due to a low white blood cell count. White blood cell counting is a specialty procedure that is usually carried out by experts and radiologists. Thanks to recent advances, image processing techniques are frequently used in biological systems to identify a wide spectrum of illnesses. In this work, image processing techniques were applied to enhance the white blood cell deep learning models' classification accuracy. To expedite the classification process, Convolutional Neural Network models were combined with Ridge feature selection and Maximal Information Coefficient techniques. These tactics successfully determined the most important characteristics. The selected feature set was then applied to the classification procedure. ResNet-50, VGG19, and our suggested model were used as feature extractors in this study. The categorizing of white blood cells was completed with an amazing 98.27% success rate. Results from the experiments demonstrated a considerable improvement in classification accuracy using the proposed Convolutional Neural Network model.

1. Introduction

White Blood Cells (WBCs) are essential components within the circulatory system of humans [1], playing a crucial role in immune defense against bacteria, viruses, and microbes [2]. WBCs counts in people usually fall between 4000 and 10,000. These counts can act as markers for different diseases or show signs of abnormalities such as persistent infections, sudden weight loss, weakness, and exhaustion. In these situations, early diagnosis becomes crucial [3]. WBCs are classified as Eosinophil, Lymphocyte, Monocyte, and Neutrophil in microscopic pictures for expert evaluation, as shown in Figure 1. This is a common way of clinical diagnosis. WBCs types can be identified with the use of microscopic imaging, albeit the process is highly dependent on the skill of the experts. This work highlights the critical relevance of feature selection in the quick and precise

identification of WBCs types utilizing a suggested method with microscopic pictures. Feature selection techniques support an intersection approach in sets, which optimizes sets generated by deep learning models.

The accurate and rapid classification of WBCs is pivotal in disease diagnosis and management, and the use of **Convolutional Neural Networks** (CNNs) based methods is recommended. While CNNs offer high accuracy, enhancing success involves developing deep features at various levels of CNN architecture. Therefore, combining feature selection methods can boost accuracy by providing more distinguishing features in a lower-dimensional space. This article introduces and evaluates such a combination, with specific goals such as assessing feature selection combinations, comparing them with simple feature combinations, and predicting the number of selected best features.

*Corresponding author: emrah.aslan@dicle.edu.tr

Received: 06.12.2023, Accepted: 28.02.2024

CNN models that have already been trained are now widely used as an effective method for differentiating distinct WBC kinds. CNNs were trained to perform this new task using transfer learning techniques. Fully automated systems were utilized in this manner. In this work, we concentrate on deep characteristics that are taken from various CNN architecture layers. A variety of feature selection techniques were used to extract the most pertinent information from two distinct pre-trained CNN models. We used pre-trained ResNet-50 and VGG19 models for transfer learning. The outcome is a totally automatic, reliable, and very accurate model for WBC classification.

The organization of the paper is as follows: Section 2 presents a literature review on WBCs studies, Section 3 introduces the data set and methods, Section 4 reports the experimental results and Section 5 concludes.

2. Literature Review

This section provides a summary of the literature on MDG classification, taking into account the dataset, methods and performance measures. There are many approaches to classify the WBC type in the literature. The most popular of these approaches are Machine Learning (ML), Fuzzy Logic, or a combination of all of them. Singh et al. proposed a CNN model for MDD classification [21]. We provide a thorough overview of the literature on WBCs categorization in this part, taking into account various datasets, approaches, and performance indicators. Using deep learning models, segmentation, pattern identification, form recognition, picture rotation methods, and feature extraction, Abbas et al. classified white blood cells data into three primary groups and seven sub-classes. Geometric Active Contours (GACs), level set approaches, edge and boundary detection, and thresholding techniques were all used in the segmentation process [4-5]. Zhao et al. demonstrated an automated recognition and classification method using microscopic images that determines the types of white blood cells by utilizing the correlation between RGB and intermediate colors. Granularity features, specifically binary rotation-invariant local binary patterns, were utilized with the Support Vector Machines (SVMs) classifier for certain WBCs types, while the CNN model and Random Forest (RF) were employed for others, resulting in a classification accuracy of 92.6% [6-7]. Habibzadeh et al.'s classification of white blood cells data consisted of three steps: preprocessing computations, a classification technique, and white blood cell identification utilizing hierarchical topological property subtraction using Inception and ResNet

architectures. Kurniadi et al. employed k-Nearest Neighbors (kNN) and XGBoost for classification, and the VGG16 model in conjunction with Local Binary Pattern (LBP) for property subtraction. 92.93% of reclassifications using test data and 90.16% of reclassifications utilizing data augmentation were successful [8-12].

Ma et al. created a classifier by combining ResNet and DC-GAN to increase the accuracy [22]. The CNN model was trained using two hundred iterations. In a study applying CNN to classify white blood cells, Şengür et al. proposed a BCC classification approach in which the "First Region of Interest" (ROI) is extracted from blood cell images in HSV space and then feature extraction is performed using ResNet50 [23]. In this study, feature extraction was performed using the Principal Component Analysis (PCA) method and classification was performed using the UKSB classifier. With this approach, an accuracy of 85.7% was achieved. Using the same dataset, Patil et al. used the Canonical Correlation Analysis (CCA) method to improve the accuracy [24, 25]. In this study, CNN models were combined to enrich the understanding of image content. Çınar et al., in a study, proposed a DL-based Hybrid CNN model for the classification of WBCs. The proposed model is based on pre-trained Alexnet and Googlenet architectures. The feature vector in the final pooling layer of both CNN architectures is combined and the resulting feature vector is classified by a Support Vector Machine [26]. In addition, Girdhar et al. proposed a CNN approach that is said to be able to classify the BKH type with much fewer iterations than other approaches [27]. Yu et al. used ResNet50, Inception V3, VGG16, VGG19, Xception software for MDD classification in their study and stated that the highest value with an accuracy rate of 88.5% among other classification methods was obtained with the CNN method [28]. Macawile et al. used the CNN techniques GoogleNet, Alexnet and ResNet-101 for MDD classification and obtained an average accuracy of 96.63% [29]. Zhao et al. presented an automatic detection and classification method for MDR data [30]. In the study, microscope images were examined and WBC types were identified by linking red, green, blue (RGB) and their intermediate colors. CNN model was used to generate features and the classification accuracy was limited to 92.6%. Razzak et al. performed segmentation and classification using the MDD dataset and used the Extreme Machine Learning (EML) method [30] in combination with CNN in the classification step [31]. The segmented cell images are masked before the feature extraction phase. Features were then extracted from each segmented cell and classification was performed with a 95.1% success rate. Hegde et al.

used both traditional image classification and CNN in their study and compared the results of these two approaches [32]. Although the results obtained were similar, it was stated that the traditional method relies heavily on segmentation and feature extraction, while CNN does not depend on these parameters. However, it was also mentioned that the CNN approach requires a large amount of labeled data and traditional image processing does not have such requirements. Considering the related studies, pre-trained CNN models have been shown to be a useful tool for differentiating different types of WBCs.

While some studies relied on handcrafted features, which can be labor-intensive, CNN-based approaches leveraged pretrained models for distinguishing WBCs types. Transfer learning techniques adapted CNNs to new tasks, resulting in fully automatic systems. However, this study emphasizes the extraction of deep features from various CNN architecture levels. The most pertinent characteristics were obtained from three pretrained CNN models, which were chosen using a variety of feature selection techniques.

3. Material and Method

3.1. WBCs Dataset

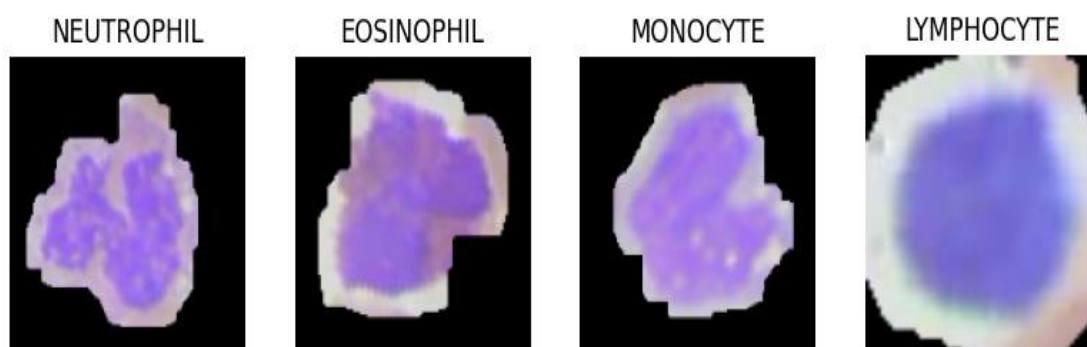


Figure 1. White Blood Cells Types [20]

3.2. Convolutional Neural Network Models

Convolutional Neural Networks (CNNs) stand out as powerful deep learning models, particularly successful in domains like image recognition. They are a specialized type of artificial neural network designed for feature identification and learning within data. What distinguishes CNNs from traditional neural networks is the inclusion of convolutional layers, which diminish the sensitivity of features to alterations like scale, translation, and rotation. Figure 2 illustrates the CNN model.

Key components of CNNs include:

This work made use of a dataset that was freely accessible and was separated into four different categories: neutrophil, lymphocyte, monocyte, and eosinophil. The dataset is available as open access on kaggle

(<https://www.kaggle.com/datasets/paultimothymooney/blood-cells>) [20]. The images in the dataset have been labelled by the experts who created the dataset. For a total of 12,435 photos, the WBCs dataset includes 3,120 images of neutrophils, 3,102 images of lymphocytes, 3,091 images of monocytes, and 3,120 images of eosinophils. Every image is saved in JPEG format, with 320×240 pixels of resolution and 24 bits of depth. All samples in the dataset underwent examination and labeling by experienced experts. To ensure efficiency in the study, an equal number of data samples, totaling 12,364 images, were maintained for each class, with 3,091 images from each category. In cases where a class had more than 3,091 images, image election was performed randomly. Additionally, the dataset was divided into training and test sets, with proportions of 70% for training and 30% for testing. This division aimed to facilitate the estimation of the proposed approach's performance on unseen data.

- Convolutional Layers: These layers execute convolution operations on input data using filters (kernels), extracting feature maps.

- Pooling Layers: Utilized to shrink the size of feature maps while retaining salient features. Max pooling is a common method of choice.

- Fully Connected Layers: Responsible for generating the CNN's output, often applied in tasks such as classification or regression.

CNNs find extensive application, especially in realms like image recognition, object detection, and facial recognition. Notably, pre-trained networks can be

repurposed effectively in various tasks through transfer learning.

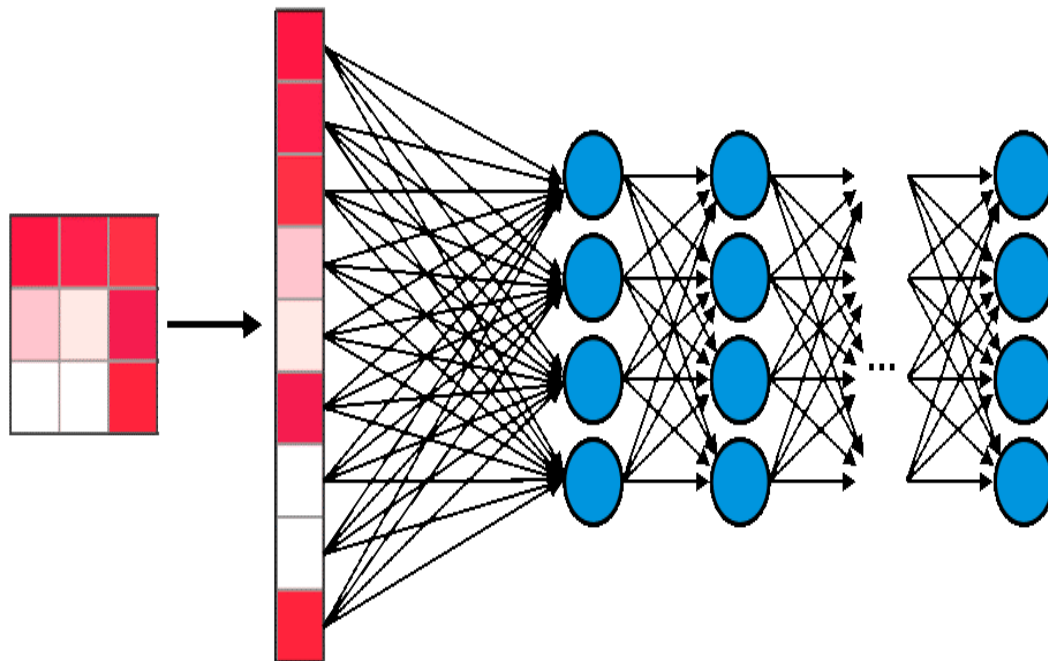


Figure 2. CNNs model.

3.3. VGG19

VGG19, a CNN improved by the Visual Geometry Group (VGG) at the University of Oxford, holds a prominent place in the realm of CNNs. As part of the VGG family, it has demonstrated significant success in various applications. VGG19, specifically, is a deep CNN composed of a total of 19 layers, featuring a distinctive architecture with key characteristics:

- Layer Structure: VGG19 comprises 16 convolutional layers and 3 fully connected layers, summing up to a total of 19 layers.

- Convolution and Pooling: Between convolutional layers, 3x3-sized filters and sequential max pooling are employed. This design enhances the network's depth and augments its capability for feature extraction.

- Fully Connected Layers: Post the convolutional layers, fully connected layers are used for the classification process, making VGG19 well-suited for classification tasks.

- Activation Functions: VGG19 typically utilizes ReLU (Rectified Linear Unit) activation functions, contributing to its overall performance.

- Total Number of Parameters: VGG19 is characterized by a large model size, indicated by a high total number of parameters. This underscores the necessity for training on substantial datasets.

VGG19 has earned recognition for its exceptional performance on the ImageNet dataset and has

excelled in the ImageNet Large Scale Visual Recognition Challenge (ILSVRC). Furthermore, its efficacy extends to transfer learning applications, where pre-trained networks can be leveraged for diverse tasks.

3.4. ResNet-50

Microsoft Research created the deep learning model ResNet-50. ResNet presents "residual learning" as a way to make deep neural network training easier. This model is designed to address challenges encountered when training large and deep neural networks. Key features of ResNet-50 include:

- Residual Blocks: ResNet incorporates residual blocks, which differ from traditional CNNs. These blocks enable "residual" learning by adding the unit's output to its input, facilitating training and reducing the issue of gradient vanishing.

- First Layer: ResNet-50 includes a convolutional layer to reduce the dimension of input data.

- Layer Structure: ResNet-50 consists of a total of 50 layers, including convolutional layers, residual blocks, and fully connected layers.

- Global Average Pooling: ResNet models often use global average pooling to reduce the feature map's size from the last convolutional layer. This can help the network learn more general and scalable features.

- Activation Functions: ReLU activation functions are commonly used.

- Total Number of Parameters: ResNet-50 is a large model with millions of parameters.

ResNet-50 has achieved significant success in the ImageNet dataset's ImageNet Large Scale Visual Recognition Challenge (ILSVRC). It is commonly used in transfer learning applications, allowing the utilization of a pre-trained network for various tasks. ResNet-50 has a deep network structure with the incorporation of residual connections, effectively addressing the challenges of backpropagation in deep architectures.

3.5. Classifier using Quadratic Discriminant Analysis

Due to its ability to complete both jobs simultaneously, Linear Discriminant Analysis (LDA) is a popular option. Discriminant analysis is important for both classification and dimensionality reduction. On the other hand, Quadratic Discriminant Analysis (QDA) offers the advantage of nonlinear data analysis. By optimizing the shared probability value across classes, QDA is a machine learning technique that generates a unique covariance matrix

for every class. However, it does not serve as a dimensionality reduction technique. Equations play a pivotal role in the classification process of QDA [13]. 'k' stands for a class in these calculations, while $\sum k$ indicates the total number of classes. π_k modifies the prevalence ratio of observations unique to each class 'k'. The equations use the observation 'x,' and QDA is used to determine the probability that 'x' is a member of class 'k'. Equation (1) is used to calculate new points using QDA using either the discriminant function or the number of posterior probabilities (δ_x). The top portion of the matrix and the covariance matrix diagonal are taken into account since each class's covariance matrix is computed separately via QDA. Where μ_k denotes a class-specific mean vector. 'p' is the input parameter for the p class prediction, and the number of QDA parameters is quadratic in p [14]. Together, these formulas strengthen QDA's ability to handle intricate data structures and perform accurate categorization.

In this study, the reason for using the QDA classifier is that it yields more successful results compared to other classifiers.

$$\delta_x = -\frac{1}{2} \log \left| \sum k \right| - \frac{1}{2} (x - \mu_k)^T \sum_k^{-1} (x - \mu_k) + \log \pi_k \tag{1}$$

3.6. Feature Selection Method

Methods for choosing features are essential in the field of machine learning because they help create a subset of more distinguishing characteristics while lowering processing costs and improving classification accuracy. These techniques are essentially made to reduce the number of dimensions in the data, which enhances the functionality of machine learning models. Using a feature selection strategy yields a new set of features, F', and a lower dimensionality, S', if the property extracted from the dataset are represented as F and the dimensionality is indicated as S, for example. The main goal is to have F' < F and S' < S. As a result, property election is frequently used to improve machine learning algorithms' efficacy and simplify data.

The Maximum Information Coefficient (MIC) is the first. MIC looks for correlations between different variables in big datasets. A statistical metric used to assess the relationship between two variables is called mutual information. It assesses the probability of two variables occurring together, considering both linear and nonlinear relationships. The method selects variables with the maximum information

content. The variables in Equation (2) are indicated by the parameters X and Y. In order to minimize any irregularities (entropy) between variables, normalization is carried out by dividing by the largest value within that set if the paired variables in the dataset disagree, as shown in Equation (3). These steps collectively contribute to the effectiveness of the MIC method in selecting informative features for improved machine learning outcomes.

$$H(X_b) = H(Y_b) = H(X_b, Y_b) \tag{2}$$

$$I(X; Y) = H(X) + H(Y) - H(X, Y) \tag{3}$$

A statistical technique for examining data based on multivariate cause-and-effect relationships is ridge regression. This method is advised as it can yield variance rates that are lower than those obtained by the Least Squares Approach. Ridge regression masks any problems by decreasing the size of the regression coordinates. That's the reason it works so well. Equation (4) contains the ridge regression formula. The constant variable "z" in this equation has values ranging from 0 to 1. Equation (4) uses the parameter 'T', the unit matrix, to represent the identity matrix. Furthermore, each feature in the dataset has plane coordinates that correlate to the

parameter's "X" and "Y". Ridge regression is particularly useful in scenarios where the least squares method may encounter issues such as multicollinearity, providing a more robust approach to regression analysis.

$$\text{Ridge} = (XX^T + zI)^{-1}X^TY \quad (4)$$

Where, represents the Ridge regression coefficient vector, 'X' is the matrix of input features, 'Y' is the output vector, 'I' is the identity matrix, and 'z' is the regularization parameter. The use of Ridge regression is especially advantageous when dealing with datasets that exhibit multicollinearity, enhancing the stability and performance of the regression analysis. The objective was to compare these two strategies' efficacy with three other feature selection methods, namely F Regression, Recursive Feature Elimination (RFE), and Linear Regression. The objective was to determine which two of these five feature selection techniques performed the best. The BKH dataset was subjected to experimental investigations, which demonstrated that the MIC and Ridge Regression techniques performed better than the other feature selection algorithms. The reference section contains the source code for various feature selection techniques. Efficient features were extracted by applying separate applications of MIC and Ridge Regression to the merged feature sets. This strategy leveraged the agreement between the best-performing MIC and Ridge Regression techniques to improve the robustness and dependability of the chosen features.

4. Proposed Method

The proposed method comprises three main steps, as outlined below:

1. Feature Extraction using CNN Models:

- In the initial step, CNN models VGG19 and ResNet-50 are employed as property extractors.

- Features obtained from the layers of CNN models are combined, creating a comprehensive feature set.

2. Ridge Regression and MIC-Based Feature Selection:

The use of feature selection techniques, particularly Ridge Regression and MIC, is done in the second stage. The most illuminating aspects from the combined feature set are chosen and kept using these techniques.

3. Combination of Classification and Feature Selection Techniques:

- A variety of feature selection techniques are used in the third phase.

- This combined feature set uses the intersecting features that were chosen using the Ridge Regression and MIC techniques.

- The selected features are then classified using the QDA.

The overall design and flow of the proposed approach are visualized in Figure 3, illustrating how the CNN models, feature selection methods, and classification steps are intricately connected to achieve an effective and robust solution. We trained VGG19 and ResNet-50 with transfer learning and combined the results with our proposed model. Table 1 shows the hyperparameters of the VGG19 and ResNet-50 models. ReLU was used as the activation function and Adam as the optimiser in the models.

Table 1. VGG19 and ResNet-50 model hyperparameters

Hyperparameters	Value
Activation	ReLU
Optimizer	Adam
Loss	categorical_crossentropy
Pooling	max
Learning_Rate	0,01
Epochs	50
Batch_Size	32
Dropout	0,2

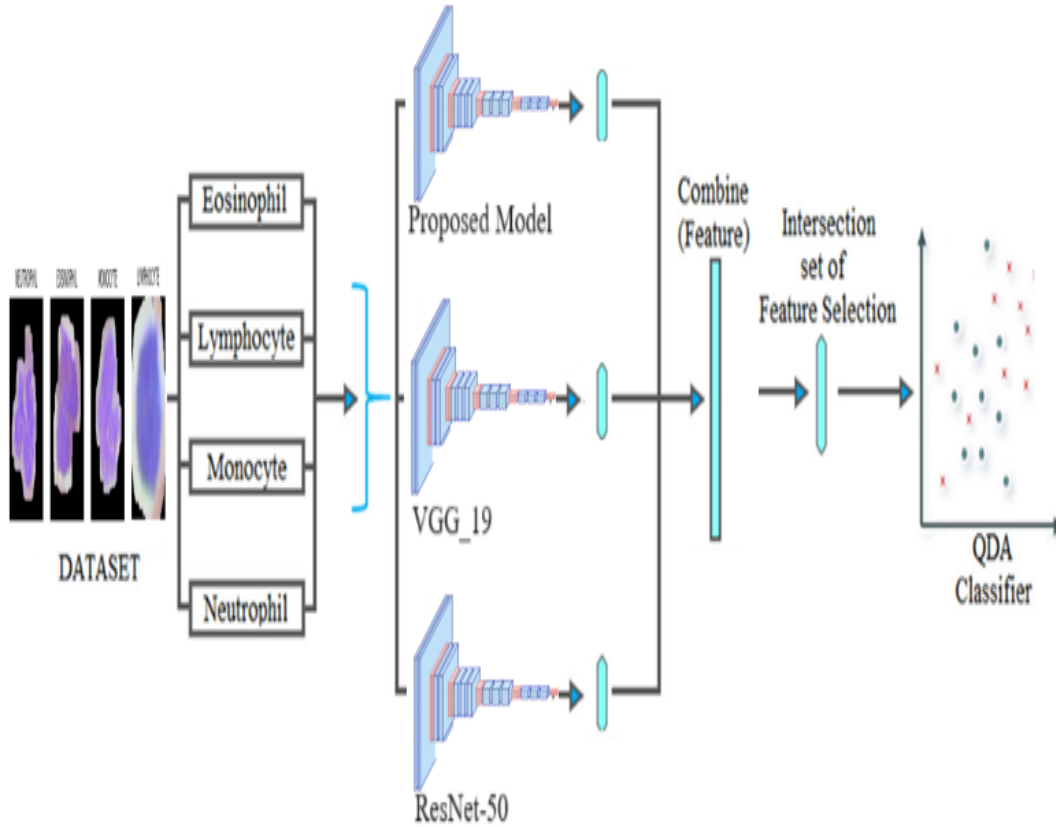


Figure 3. Model design of the proposed model

The images used to validate the proposed approach were obtained from an openly accessible dataset. The dataset was randomly divided for training, with 80% of the data used for training and 20% for test samples from each class. Additionally, the training dataset (randomly selected) was further divided into 90% for training and 10% for training validation purposes. Randomly selected cell samples from the dataset are provided in Figure 4.

The proposed approach unfolds in three key stages: data preprocessing, feature extraction, and classification. These stages are visually depicted in

Table 2. For a more detailed overview and understanding of the proposed approach, the block diagram is provided in Figure 5. This diagram illustrates the interconnected flow of processes, emphasizing the progression from data preprocessing through feature extraction to the final classification step. The block diagram serves as a comprehensive visual representation of the methodology, aiding in the comprehension of the overall approach and its sequential execution of essential tasks.

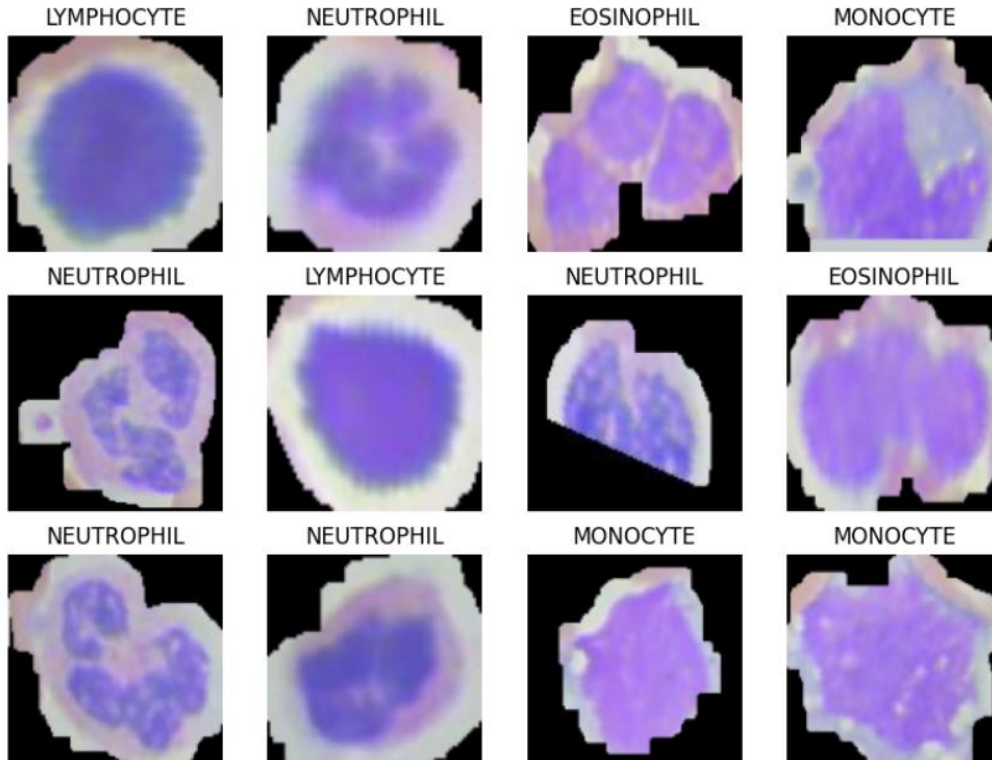


Figure 4. Dataset [20]

Table 2. Details of the proposed method

Layer	Output Shape	Parameter
Conv2d (Conv2D)	(None, 118, 118, 64)	1792
Max_pooling2d (Maxpooling2D)	(None, 59, 59, 64)	0
Dropout (Dropout)	(None, 59, 59, 64)	0
Conv2d_1 (Conv2D)	(None, 57, 57, 128)	73856
Max_pooling2d_1 (Maxpooling2D)	(None, 28, 28, 128)	0
Dropout_1 (Dropout)	(None, 28, 28, 128)	0
Conv2d_2 (Conv2D)	(None, 26, 26, 256)	295168
Max_pooling2d_2 (Maxpooling2D)	(None, 13, 13, 256)	0
Dropout_2 (Dropout)	(None, 13, 13, 256)	0
Flatten (Flatten)	(None, 43264)	0
Dense (Dense)	(None, 1024)	44303360
Dropout_3 (Dropout)	(None, 1024)	0
Dense_1 (Dense)	(None, 4)	4100
Total parameters:	44678276 (170.43 MB)	
Trainable parameters:	44678276 (170.43 MB)	
Non-trainable parameters:	None	

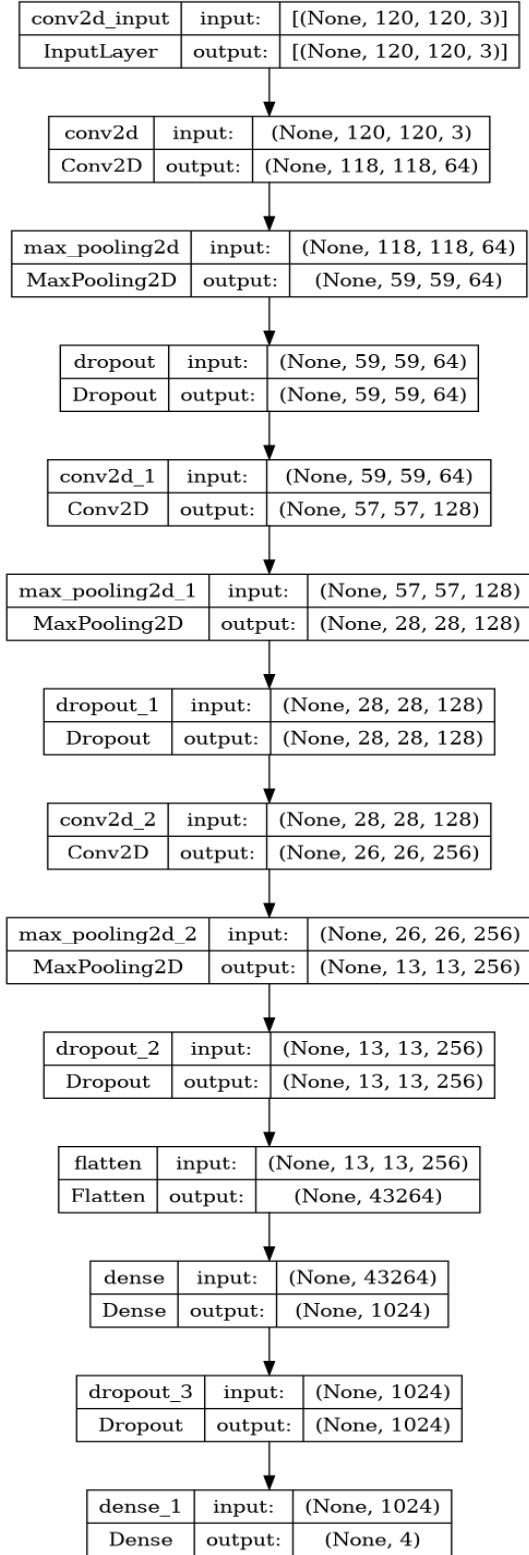


Figure 5. Flow diagram of the proposed method

5. Experimental Results

In this section, the outcomes derived from the materials and methods outlined in the preceding section are presented.

Important measures, such as sensitivity, specificity, F1-score, and accuracy, are used to assess the proposed model. The parameters true positive (TP), true negative (TN), false positive (FP), and false negative (FN) are the foundation of these measures.

The parameters in these equations are defined as follows:

- True Positive (TP): Instances that the model accurately classified as positive.
- True Negative (TN): Examples that the model accurately classified as negative.
- False Positive (FP): Cases that the model mistakenly classified as positive.
- False Negative (FN): Examples that the model misinterpreted as negative.

These metrics provide a comprehensive evaluation of the model's performance, considering both positive and negative classifications. The F1-score strikes a compromise between precision and recall, while sensitivity and specificity provide information about the model's capacity to properly detect positive and negative examples, respectively. The accuracy measure offers a general evaluation of how accurate the model's predictions are.

$$Accuracy = \frac{TP + TN}{(TP + TN + FP + FN)} \tag{9}$$

$$Recall = \frac{TN}{(TP + FN)} \tag{10}$$

$$Specificity = \frac{TN}{(TN + FP)} \tag{11}$$

$$Precision = \frac{TP}{(TP + FP)} \tag{12}$$

$$F_1 = 2 * \frac{Precision * Recall}{(Precision + Recall)} \tag{13}$$

In this step, considering the classification performance metrics (sensitivity, precision, etc.), the overall accuracy rate is 98.27%. The proposed confusion matrix is presented in Figure 6, and the performance curve graph is provided in Figure 7. Additionally, intersecting features have been extracted using feature selection methods. This indicates the selection of more intersecting features. The model's ability to classify blood cells is shown in Figure 8.

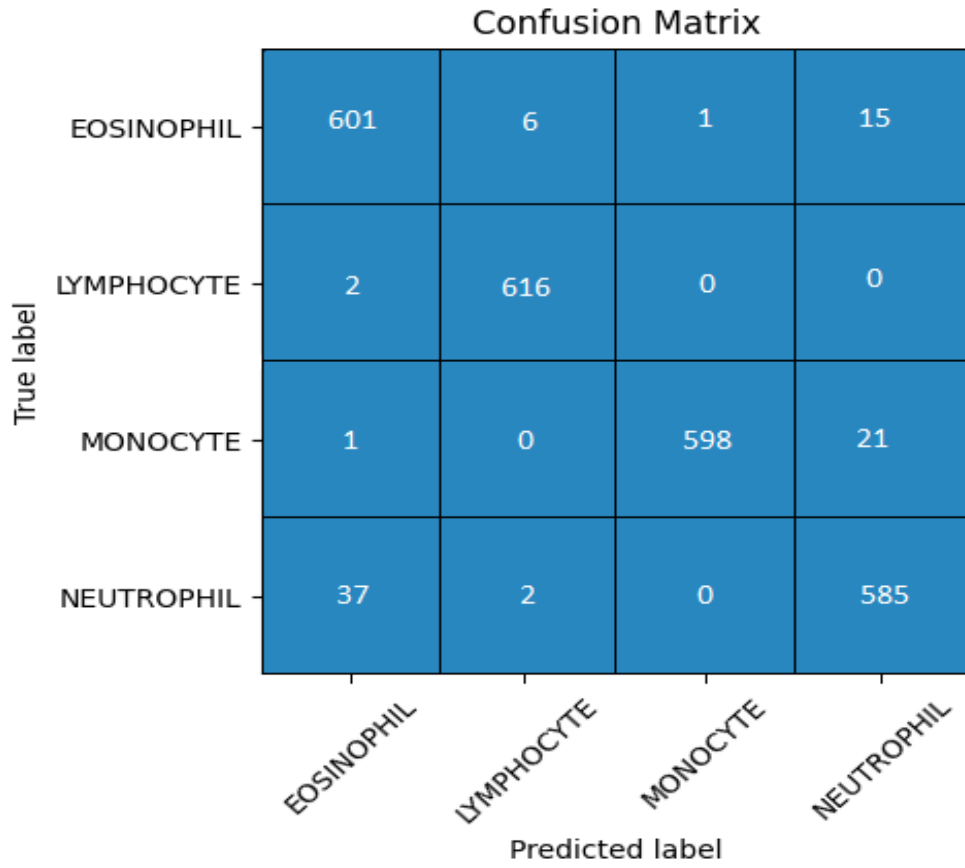


Figure 6. Confusion matrix of the proposed model

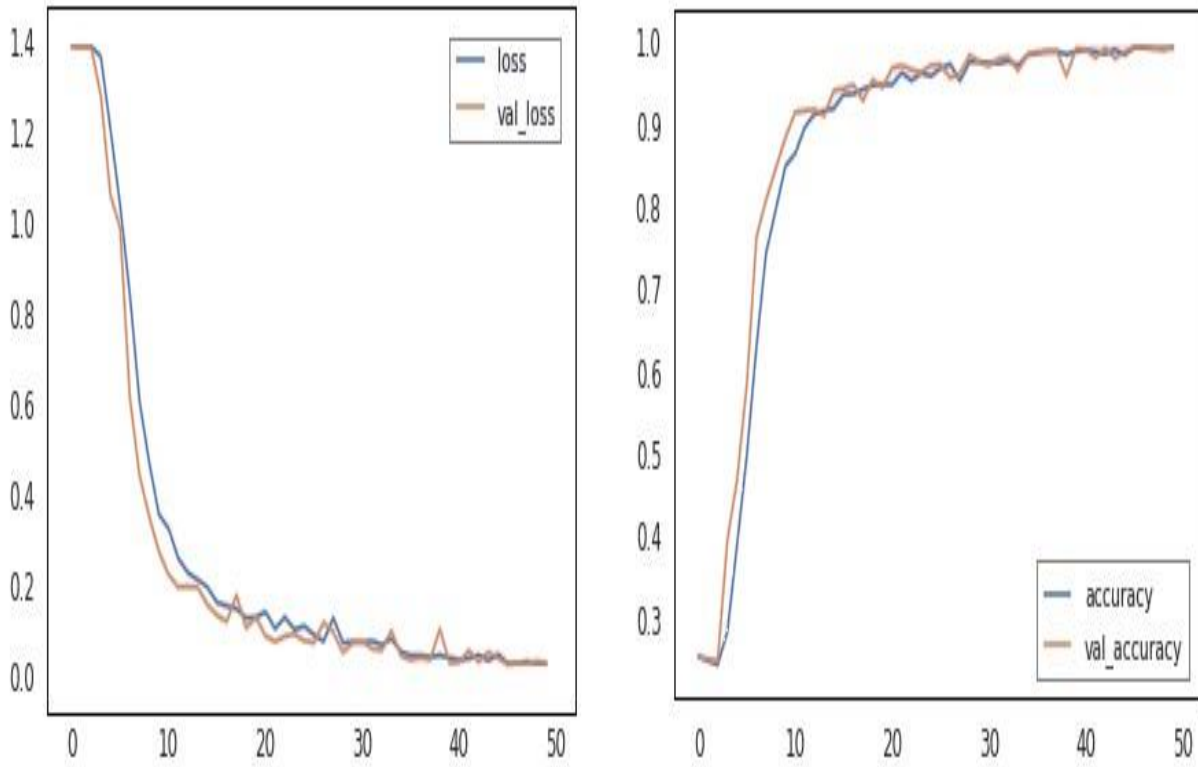


Figure 7. Performance graph of the proposed model

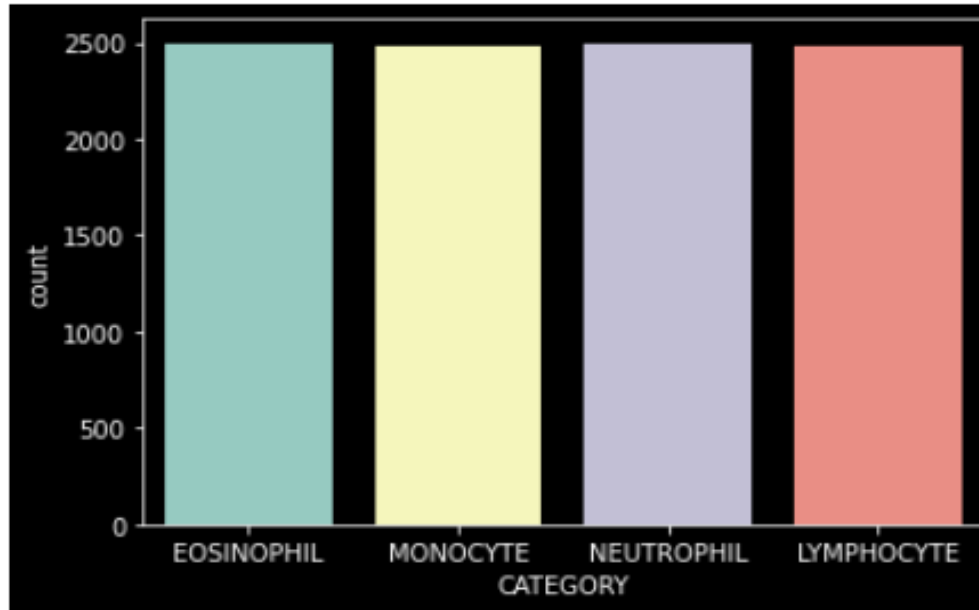


Figure 8. Categorization capability of the model

According to the data presented in Table 3, our developed method can determine the features of the input image by following an adaptive learning process. This enables effective classification without being tightly dependent on cell segmentation or feature design. Traditional methods are known to often cause imbalance issues, which can hinder the classifier from accurately predicting cell abnormalities. Our method can effectively address this imbalance issue. Additionally, our model, when

compared to classical neural network models like ResNet-50 and VGG-19, appears to fully utilize the spatial and temporal information of image features. In conclusion, our new method may have significant application potential in the classification of blood cell images. Overall, our study, with its proposed approach and sufficient image count in the dataset, provides reliable results, being both innovative and trustworthy.

Table 3. Comparison of the results of the model with the results in the literature.

Study	Methods	Classification Accuracy (%)
Kumar et al. [17]	Multi SVM	75.88
Sedat et al. [18]	Principal Component Analysis	95.79
Li et al. [19]	Dual-ThresholdMethod	91.20
Proposed Model	ResNet-50, VGG19, QDA	98.27

6. Conclusion

In this study evaluated the efficacy of a variety of feature selection methods for the categorization of Eosinophils, Lymphocytes, Monocytes, and Neutrophils utilizing Eosinophil-Specific Antibodies. The suggested method combines features taken from ResNet-50, VGG19's 1000-feature layers, and a specially created model. Ridge and MIC property election approaches were used to the merged feature collection. The classification results were notably improved by the intersecting features that were obtained from the MIC and Ridge approaches, indicating the additional benefit of

integrating feature selection techniques. Using the Quadratic Discriminant Analysis (QDA) approach, the experimental findings demonstrated a remarkable overall accuracy rate of 98.27% for CNN classification. With 97.48% accuracy for Eosinophil, 99.58% for Lymphocyte, 99.05% for Monocyte, and 96.96% for Neutrophil, the CNN kinds' accuracy results were particular and impressive. This demonstrates the model's consistent performance in a range of cell types. Preprocessing procedures are expected to be added to the suggested technique for future research. With this evolution, the model's performance is intended to be further optimized,

which may help in the development of high-performance computer-aided systems for future medical imaging jobs. The work establishes the groundwork for future developments in automated cell categorization, especially with regard to image analysis and medical diagnostics.

Conflict of Interest Statement

There is no conflict of interest between the authors.

Statement of Research and Publication Ethics

The study is complied with research and publication ethics

References

- [1] G.C. Kabat, M.Y. Kim, J.A.E. Manson, L. Lessin, J. Lin, S. Wassertheil-Smoller, T.E. Rohan, "White blood cell count and total and cause-specific mortality in the women's health initiative," *Am. J. Epidemiol.*, vol. 186, pp. 63–72, 2017. (<http://dx.doi.org/10.1093/aje/kww226>)
- [2] A. Mbanefo and N. Kumar, "Evaluation of malaria diagnostic methods as a key for successful control and elimination programs," *Trop Med Infect Dis*, vol. 5, no. 2, p. 102, 2020.
- [3] S. Nema, M. Rahi, A. Sharma, and P.K. Bharti, "Strengthening malaria microscopy using artificial intelligence-based approaches in India," *Lancet Reg Health - Southeast Asia*, vol. 5, p. 100054, 2022.
- [4] World Health Organization, *Malaria microscopy quality assurance manual-version 2*, 2021.
- [5] K.A.L.-D. ulaimi, I. Tomeo-Reyes, J. Banks, and V. Chandran, "Evaluation and benchmarking of level set-based three forces via geometric active contours for segmentation of white blood cell nuclei shape," *Comput. Biol. Med.*, vol. 116, p. 103568, 2020. [[doi:10.1016/j.combiomed.2019.103568](https://doi.org/10.1016/j.combiomed.2019.103568)](<http://dx.doi.org/10.1016/j.combiomed.2019.103568>)
- [6] J. Zhao, M. Zhang, Z. Zhou, J. Chu, and F. Cao, "Automatic detection and classification of leukocytes using convolutional neural networks," *Med. Biol. Eng. Comput.*, vol. 55, pp. 1287–1301, 2017. [[doi:10.1007/s11517-016-1590-x](https://doi.org/10.1007/s11517-016-1590-x)](<http://dx.doi.org/10.1007/s11517-016-1590-x>)
- [7] P. Chun, I. Ujike, K. Mishima, M. Kusumoto, and S. Okazaki, "Random forest-based evaluation technique for internal damage in reinforced concrete featuring multiple nondestructive testing results," *Constr. Build. Mater.*, vol. 253, p. 119238, 2020. [[doi:10.1016/j.conbuildmat.2020.119238](https://doi.org/10.1016/j.conbuildmat.2020.119238)](<http://dx.doi.org/10.1016/j.conbuildmat.2020.119238>)
- [8] A. Barai, M.F. Faruk, S.M. Shuvo, A.Y. Srizon, S.M. Hasan, and A. Sayeed, "A Late Fusion Deep CNN Model for the Classification of Brain Tumors from Multi-Parametric MRI Images," in *2023 International Conference on Next-Generation Computing, IoT and Machine Learning (NCIM)*, Gazipur, Bangladesh, 2023, pp:1-6. <https://doi.org/10.1109/NCIM59001.2023.10212729>.
- [9] N. Mahajan and H. Chavan, "MRI Images Based Brain Tumor Detection Using CNN for Multiclass Classification," in *2023 3rd Asian Conference on Innovation in Technology (ASIANCON)*, Ravet IN, India, 2023, pp. 1-5. (<https://doi.org/10.1109/ASIANCON58793.2023.10270492>)
- [10] K. Kaplan, Y. Kaya, M. Kuncan, M.R. Minaz, and H.M. Ertunç, "An improved feature extraction method using texture analysis with LBP for bearing fault diagnosis," *Appl. Soft Comput.*, vol. 87, p. 106019, 2020. [[doi:10.1016/j.asoc.2019.106019](https://doi.org/10.1016/j.asoc.2019.106019)](<http://dx.doi.org/10.1016/j.asoc.2019.106019>)
- [11] R. Singh, A. Sharma, N. Sharma, and R. Gupta, "Impact of Adam, Adadelta, SGD on CNN for White Blood Cell Classification," in *2023 5th International Conference on Smart Systems and Inventive Technology (ICSSIT)*, Tirunelveli, India, 2023, pp. 1702-1709. [[doi:10.1109/ICSSIT55814.2023.10061068](https://doi.org/10.1109/ICSSIT55814.2023.10061068)](<http://dx.doi.org/10.1109/ICSSIT55814.2023.10061068>)
- [12] S. Montaha, S. Azam, A. Rafid, M. Hasan, Z. Karim, and A. Islam, "TimeDistributed-CNNLSTM: A Hybrid Approach Combining CNN and LSTM to Classify Brain Tumor on 3D MRI Scans Performing Ablation Study," *IEEE Access*, vol. 10, pp. 60039-60059, 2022. [[doi:10.1109/ACCESS.2022.3179577](https://doi.org/10.1109/ACCESS.2022.3179577)](<https://doi.org/10.1109/ACCESS.2022.3179577>)
- [13] S. Saeedi, S. Rezayi, H. Keshavarz, and S. R Niakan Kalhori, "MRI-based brain tumor detection using convolutional deep learning methods and chosen machine learning techniques," *BMC Med Inform Decis Mak*, vol. 23, no. 1, p. 16, Jan. 23, 2023. [[doi:10.1186/s12911-023-02114-6](https://doi.org/10.1186/s12911-023-02114-6)](<https://doi.org/10.1186/s12911-023-02114-6>)

- [14] I.M. Baltruschat, H. Nickisch, M. Grass, T. Knopp, and A. Saalbach, "Comparison of deep learning approaches for multi-label chest X-ray classification," *Sci. Rep.*, vol. 9, p. 6381, 2019. [doi:10.1038/s41598-019-42294-8](http://dx.doi.org/10.1038/s41598-019-42294-8)
- [15] H.P. Beck, "Digital microscopy and artificial intelligence could profoundly contribute to malaria diagnosis in elimination settings," *Front Artif Intell*, vol. 5, p. 510483, 2022.
- [16] Y. Kumar, A. Koul, and S. Mahajan, "A deep learning approaches and fastai text classification to predict 25 medical diseases from medical speech utterances, transcription and intent," *Soft Comput*, vol. 26, no. 17, pp. 8253–8272, 2022.
- [17] P.S. Kumar and S. Vasuki, "Automated diagnosis of acute lymphocytic leukemia and acute myeloid leukemia using multi-SV," *Journal of Biomedical Imaging and Bioengineering*, vol. 1, no. 1, pp. 20–24, 2017.
- [18] S. Nazlibilek, D. Karacor, T. Ercan, M.H. Sazli, O. Kalender, and Y. Ege, "Automatic segmentation, counting, size determination and classification of white blood cells," *Measurement*, vol. 55, pp. 58–65, 2014. (https://doi.org/10.1016/j.measurement.2014.04.008)
- [19] Y. Li, R. Zhu, L. Mi, Y. Cao and D. Yao, "Segmentation of White Blood Cell from Acute Lymphoblastic Leukemia Images Using Dual-Threshold Method," *Computational and Mathematical Methods in Medicine*, pp. 1–12, 2016. [doi:10.1155/2016/9514707](https://doi.org/10.1155/2016/9514707)
- [20] P. Mooney., Kaggle Dataset, Blood Cell Images, 14 March 2018 [Online] Available: <https://www.kaggle.com/datasets/paultimothymooney/blood-cells>.
- [21] I. Rojas, O. Valenzuela, F. Rojas, ve F. Ortuño, "Bioinformatics and Biomedical Engineering: 7th International Work-Conference. Proceedings 2019; Part I," (11465).
- [22] L. Ma, R. Shuai, X. Ran, W. Liu, ve C. Ye, "Combining DC-GAN with ResNet for blood cell image classification," *Medical & biological engineering & computing*, vol 58, no. 6, pp. 1251-1264, 2020.
- [23] A. Şengür, Y. Akbulut, Ü. Budak, ve Z. Cömert, "White blood cell classification based on shape and deep features," *International Artificial Intelligence and Data Processing Symposium (IDAP)*, pp. 1-4, 2019.
- [24] A. M. Patil, M. D. Patil, ve G. K. Birajdar, "White blood cells image classification using deep learning with canonical correlation analysis," *IRBM*, vol 42, no. 5, pp. 378-389, 2021.
- [25] A. Çınar ve S. A. Tuncer, "Classification of lymphocytes, monocytes, eosinophils, and neutrophils on white blood cells using hybrid Alexnet-GoogleNet-SVM," *SN Applied Sciences*, vol 3, no. 4, pp. 1-11, 2021.
- [26] A. Girdhar, H. Kapur, ve V. Kumar, "Classification of White blood cell using Convolution Neural Network," *Biomedical Signal Processing and Control*, vol 71, no. 103156, 2022.
- [27] W. Yu, J. Chang, C. Yang, L. Zhang, H. Shen, Y. Xia, ve J. Sha, "Automatic classification of leukocytes using deep neural network," *12th international conference on ASIC (ASICON)*, pp. 1041-1044, 2017.
- [28] M. J. Macawile, V. V. Quiñones, A. Ballado, J. D. Cruz, ve M. V. Caya, "White blood cell classification and counting using convolutional neural network," *3rd International conference on control and robotics engineering (ICCRE)*, pp. 259-263, 2018.
- [29] J. Zhao, M. Zhang, Z. Zhou, J. Chu, ve F. Cao, "Automatic detection and classification of leukocytes using convolutional neural networks," *Medical & biological engineering & computing*, vol 55, no. 8, pp. 1287-1301, 2017.
- [30] Y. Ming, E. Zhu, M. Wang, Y. Ye, X. Liu, ve J. Yin, "DMP-ELMs: Data and model parallel extreme learning machines for large-scale learning tasks," *Neurocomputing*, vol 320, pp. 85-97, 2018.
- [31] M. Imran Razzak ve S. Naz, "Microscopic blood smear segmentation and classification using deep contour aware CNN and extreme machine learning," *Proceedings of the IEEE Conference on Computer Vision and Pattern Recognition Workshops*, pp. 49-55, 2017.
- [32] R. B. Hegde, K. Prasad, H. Hebbar, ve B. M. K. Singh, "Comparison of traditional image processing and deep learning approaches for classification of white blood cells in peripheral blood smear images," *Biocybernetics and Biomedical Engineering*, vol 39, no. 2, pp. 382-392, 2019.